

Numerical modeling of sedimentation and flushing at the Paute-Cardenillo Reservoir

L. G. Castillo¹, M. A. Álvarez² and J. M. Carrillo³

¹Hidr@m Group, Department of Civil Engineering, Universidad Politécnica de Cartagena, Paseo Alfonso XIII, 52, 30203, Cartagena, Spain. PH (+34) 968327012; FAX (+34) 968338805; email: luis.castillo@upct.es

²GEAMA Group, Centro de Innovación en Edificación e Enxeñería Civil, Universidade da Coruña, Campus de Elviña, s/n 15071, A Coruña, Spain. PH (+34) 981 167000; FAX (+34) 981167170; email: manuelali.alvarez@usc.es

³Hidr@m Group, Department of Civil Engineering, Universidad Politécnica de Cartagena, Paseo Alfonso XIII, 52, 30203, Cartagena, Spain. PH (+34) 868071289; FAX (+34) 968338805; email: jose.carrillo@upct.es

ABSTRACT

The study analyzes the expected changes in the Paute River in Ecuador as a result of the construction of the Paute-Cardenillo Dam (owned by Celec Ep-Hidropaute). This dam will integrate the National Electric System of Ecuador with a total electricity installed capacity of 600 MW which will produce 13000 GWh per year. Given that the project must remain viable throughout its useful life, the operational rules at the reservoir are required to include sedimentation effects. Sediment transport and flushing are studied by using four complementary procedures: empirical formulae, one-dimensional simulations (time required for sediment level reaches the height of the bottom outlets), two-dimensional simulations (flushing) and three-dimensional simulations (detail of the sediment transport through bottom outlet).

MAIN CHARACTERISTICS OF THE PROJECT

The study zone is situated in the Paute River basin in Ecuador to 23 km downstream from the Amaluza Dam. The area to be analyzed is of 275 km² of draining surface and the average slope of the river reach is 0.05.

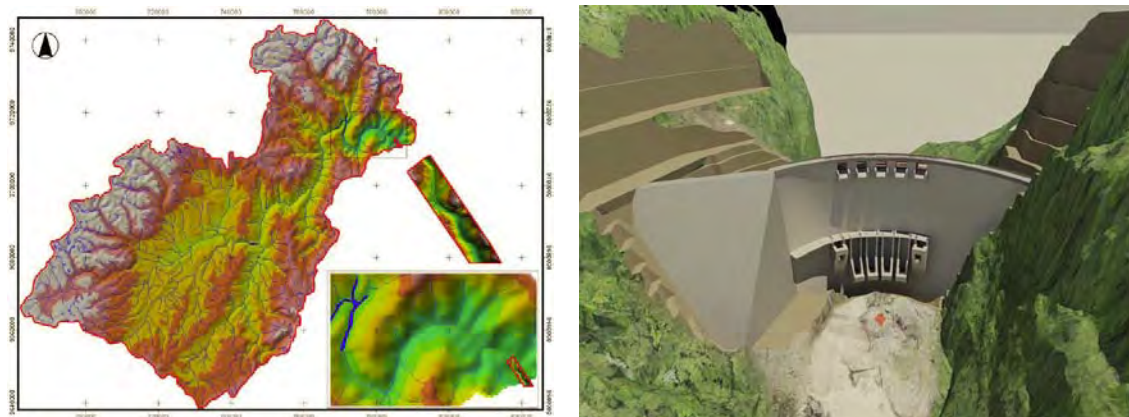


Figure 1. (a) Zone of study in Paute River basin. (b) Paute-Cardenillo Dam.

Paute-Cardenillo is a double curvature arch dam with a maximum height of 135 m to the foundations. The top level is located at 926 meters. The reservoir has a length of 2.98 km, with normal maximum water level being located at 924 meters.

Figure 2 shows the sieve curves obtained at three sites of the river and the mean curve used in the calculations. The grain-size distribution of the mean curve have the following characteristic diameters: $D_{50} = 0.15$ m, $D_{65} = 0.19$ m, $D_{84} = 0.225$ m, $D_{90} = 0.24$ m and $D_m = 0.124$ m.

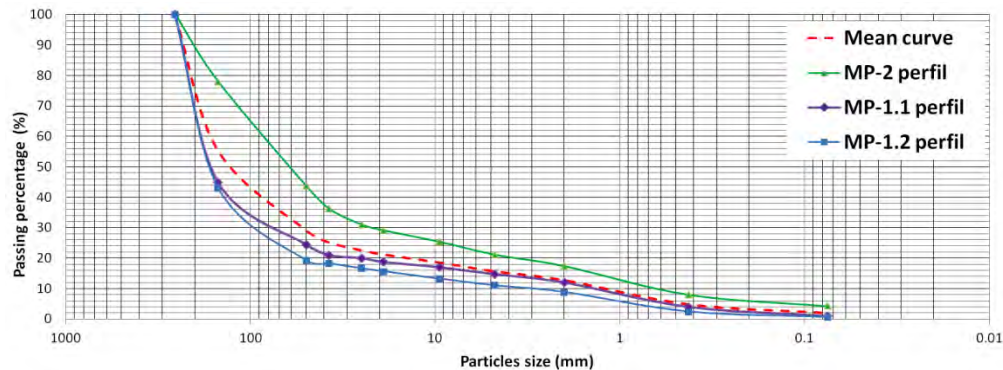


Figure 2. Sieve curves of three sites of the river and the sieve mean curve.

The total bed load (excluding wash load) was determined as $1.75 \text{ Mm}^3/\text{year}$ and the maximum volume of the reservoir 12.33 Mm^3 . In order to prevent the deposition of sediments into the reservoir, periodic discharges of bottom outlet or "flushing" have been proposed. These operations should be able to remove the sediments, avoiding the advance of the delta from the tail of the reservoir.

Initial studies indicate that the minimum flow evacuated by the bottom outlet to achieve an efficient flushing should be at least twice the annual mean flow ($Q_{ma}=136.3 \text{ m}^3/\text{s}$). For the safe side, a flow of $408.9 \text{ m}^3/\text{s}$ ($3Q_{ma}$) was adopted.

SEDIMENT TRANSPORT FORMULAE

Sediment transport may be divided into the following: wash load (very fine material transported in suspension), and total bed transport (bed sediment transported and/or in suspension, depending on the sediment size and flow velocity). The main properties of sediment and its transport are the following: the particle size, shape, density, sedimentation velocity, porosity and concentration.

Estimate of the Manning resistance coefficient. The calculation of the flow characteristics depends mainly on the resistance coefficient, hydraulic radius and longitudinal slope. Following the methodology applied in Castillo et al. (2009), four aspects were checked to determine hydraulic characteristics of the flow: macro roughness, bed form resistance, hyper concentrated flow, and bed armoring phenomenon.

Ten formulae were applied for estimation of the roughness coefficient: Strickler (1923), Limerinos (1970), Jarret (1984), Bathurst (1984), van Rijn (1987), Fuentes and Aguirre-Pe (1991), García-Flores (1996), Grant (1997), Fuentes and Aguirre-Pe (2000) and Bathurst (2002). These formulae are calculated by coupling iteratively the hydraulic characteristics with the sediment transport.

A macro roughness behavior may be identified in all the flows analyzed, which also present the armoring phenomenon. This leads to a significant increase in the various Manning coefficients. The calculation of these coefficients was carried out in a section type, through an iterative procedure by using

the formulation of Fuentes and Aguirre-Pe et al. (2000). Figure 3 shows the Manning coefficients for the flow rates.

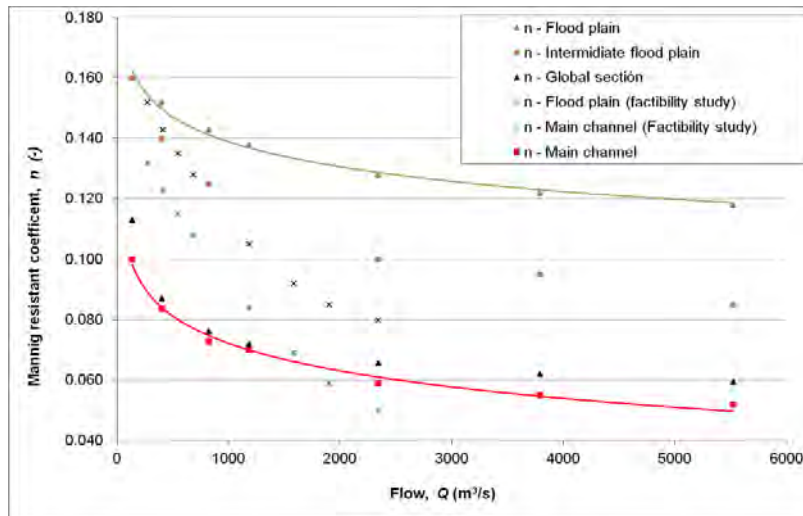


Figure 3. Manning resistance coefficients in the main channel and floodplain.

Estimation of sediment transport. Fourteen formulations of sediment transport capacity were used: Meyer-Peter and Müller (1948), Einstein and Brown (1950), Einstein and Barbarrosa (1952), Colby (1964), Engelund and Hansen (1967), Yang, C.T. (1976), Parker et al. (1982), Smart and Jaeggi (1983), Mizuyama and Shimohigashi (1985), van Rijn (1987), Bathurst et al. (1987), Ackers and White (1990), Aguirre-Pe et al. (2000) and Yang, S. (2005). From these, the formulations that fell within a range of the mean value ± 1 standard deviation were selected. Figure 4 indicates that the transport capacity could vary between 1 and 100 t/s, if the mean values of the analyzed reach are considered. However, these values are reduced between 0.5 and 10 t/s when the river complete reach is considered (erosion and sedimentation processes are simulated). Finally, the net sediment transport in dam site was only 0.2 t/s.

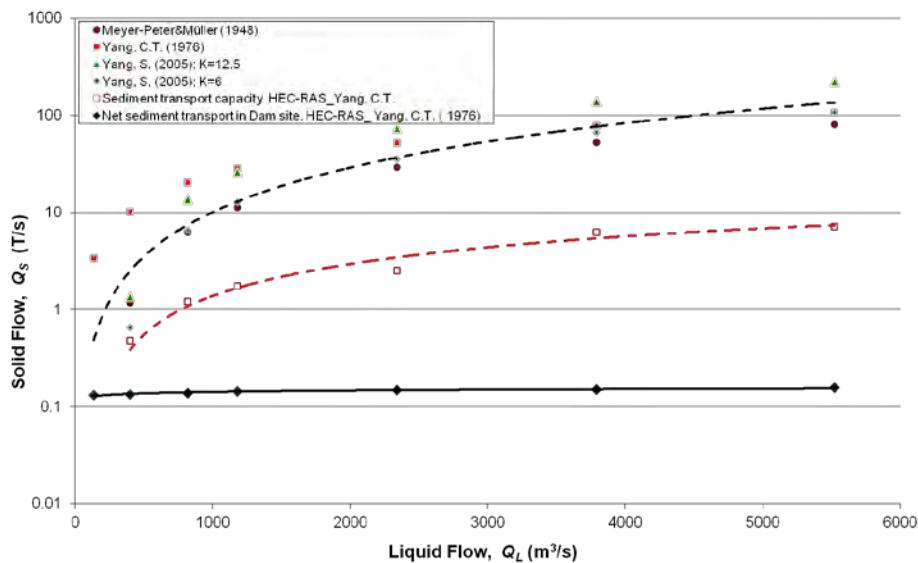


Figure 4. Sediment transport capacity (reach mean values), sediment transport (simulation of all reach) and net sediment transport in dam site.

From the expression offered by Einstein-Barbarossa (1952), the ratio of total bed transport and suspension transport was determined. These results (Figure 5) constitute an upper envelope of the sediment transport capacity, since in the calculations uniform flow, a section type and an average slope of the analyzed reach were considered. This procedure allowed an estimate of the resistant coefficients.

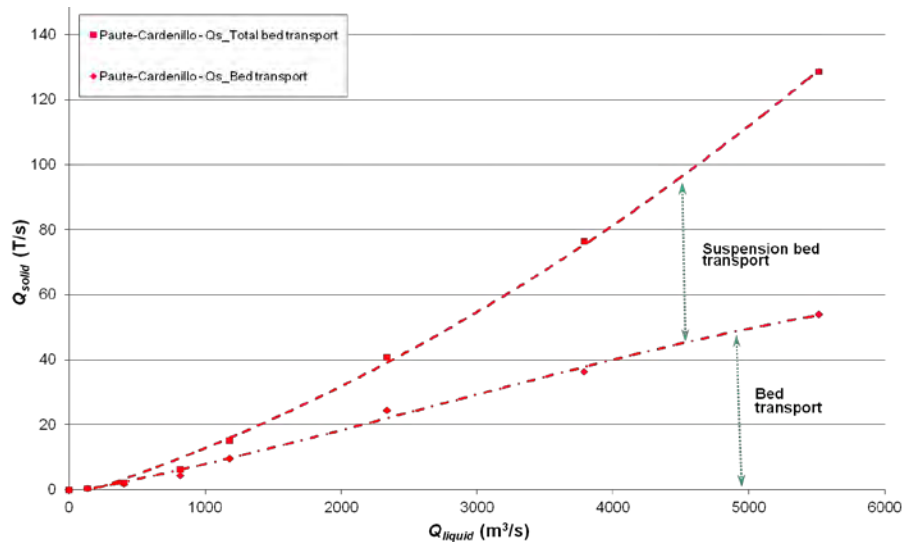


Figure 5. Solid flow in function of liquid flow.

RESERVOIR SEDIMENTATION

The time required for sediment level to reach the height of the bottom outlets (elevation 827 m) operating at reservoir levels was analyzed. Simulations were carried out with the one-dimensional HEC-RAS 4.1 program which employs a continuity equation of sediment. The change in the volume of sediment in a section of a river is equal to the difference between the sediment load entering and leaving at each control volume analyzed (Exner equation):

$$(1 - \lambda_p)B \frac{\partial \eta}{\partial t} = - \frac{\partial Q_s}{\partial x}$$

where B is the channel width, η the channel elevation, λ_p the porosity of the active layer, t the time, x the distance, and Q_s the sediment load transported.

Figure 6 shows the ground initial profile between the Amaluza and Paute-Cardillo dams. The input flows are the annual mean flow ($Q_{ma}=136.3 \text{ m}^3/\text{s}$) equally distributed in the first 12 km and the incorporation (2.44 km upstream from the Paute-Cardenillo Dam) of the annual mean discharge flow of the Sopladora hydroelectric power plant ($Q_{ma_sop}=209.0 \text{ m}^3/\text{s}$).

The suspended sediment concentration at the inlet section was $0.258 \text{ kg}/\text{m}^3$. This value is similar to the mean concentration at the Sopladora hydroelectric power plant. The sediment characteristic diameter in the dam emplacement was $D_{50} = 0.150 \text{ m}$. The sediment transport was calculated by considering the Meyer-Peter and Müller (1948) and Yang C.T. (1976) formulae. In addition, a reference hydrograph (three times the average annual flow), and hydrographs with different return periods, were also considered.

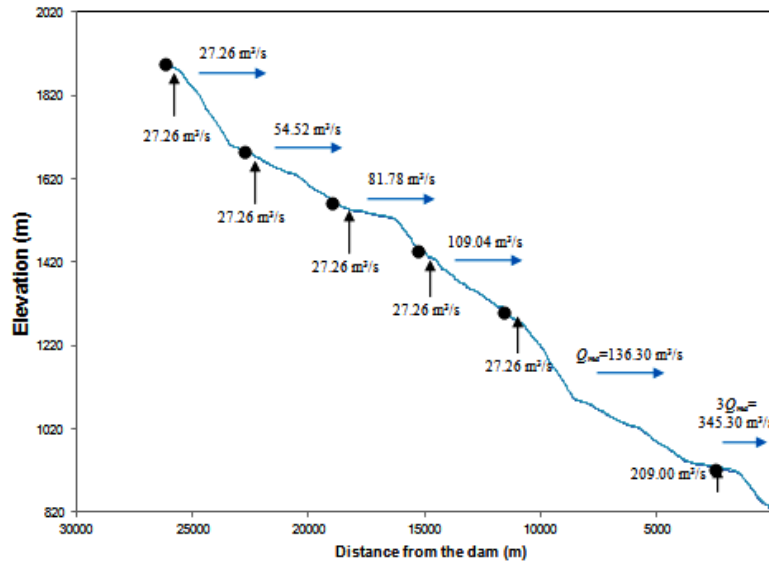


Figure 6. Ground initial profile and input flows.

Table 1 and Figure 7 show the volume of sediments in the reservoir obtained when the bottom outlet level was reached. The two transport equations, as well as various water levels in the reservoir were examined. According to the results, the volume of sediment in the reservoir rises with the increasing of the water level in the reservoir, and requires a longer duration to reach the bottom outlet elevation.

Table 1. Time required and volume of sediment when the bottom outlets are reached.

Reservoir elevation	Yang		Meyer-Peter & Müller	
	Required time (years)	Sediment volume (hm ³)	Required time (years)	Sediment volume (hm ³)
860	0.33	0.65	0.33	1.47
918	12.90	6.07	8.80	7.34

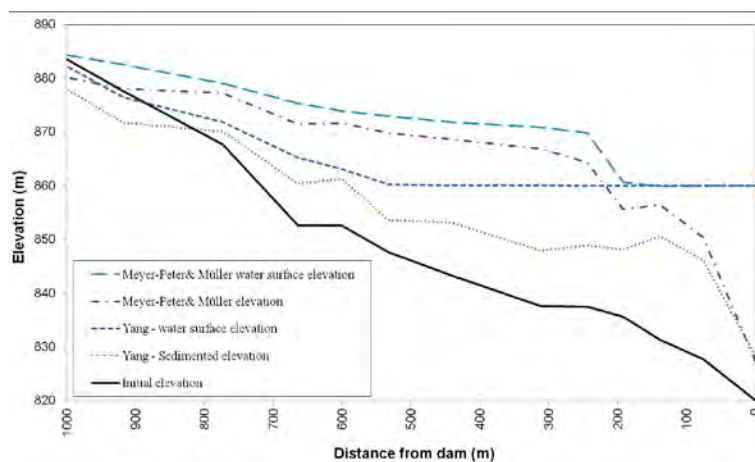


Figure 7. Original bed in the reservoir and after three months and 27 days of simulation, considering the base flow and the reservoir located at elevation 860 m.

The least favorable condition (the first one in which the sediment reaches the elevation of 827 m) was obtained with the expression of Meyer-Peter and Müller and the level of the reservoir located at 860 m, requiring a time of three months and 27 days.

FLUSING SIMULATION

Two-dimensional simulation. Since the one-dimensional model was unable to reproduce the regressive erosion of sediment in the reservoir, the flushing process was analyzed by using the Iber two-dimensional program. Iber can be divided in three modules: hydrodynamic, turbulence and sediment transport. The program uses triangular or quadrilateral elements in an unstructured mesh and finite volume scheme. The hydrodynamic module solves shallow water equations (2-D Saint-Venant equations). Diverse turbulence models with various levels of complexity can be used. The sediment transport module solves the transport equations by the Meyer-Peter and Müller expression and the evolution of the bottom elevation is calculated by sediment mass balance.

The evolution of the flushing is studied over a continuous period of 72 hours, according to the operational rules of the Paute-Cardenillo Dam. The initial condition of sedimentation profile (the lower level of the bottom outlet) was 1.47 hm^3 of sediment. The input flow was three times the annual average flow ($408.9 \text{ m}^3/\text{s}$). The suspended sediment concentration at the inlet section was $0.258 \text{ kg}/\text{m}^3$. This value was obtained from the flow drained by the upstream Sopladora hydroelectric power plant ($209 \text{ m}^3/\text{s}$) which had an mean concentration of $0.250 \text{ kg}/\text{m}^3$. Figure 8 shows the profiles of the sediment at the reservoir for times during the flushing operation. The initial water level at the reservoir was 860 m. Effective flushing was observed during the operation of the bottom outlets.

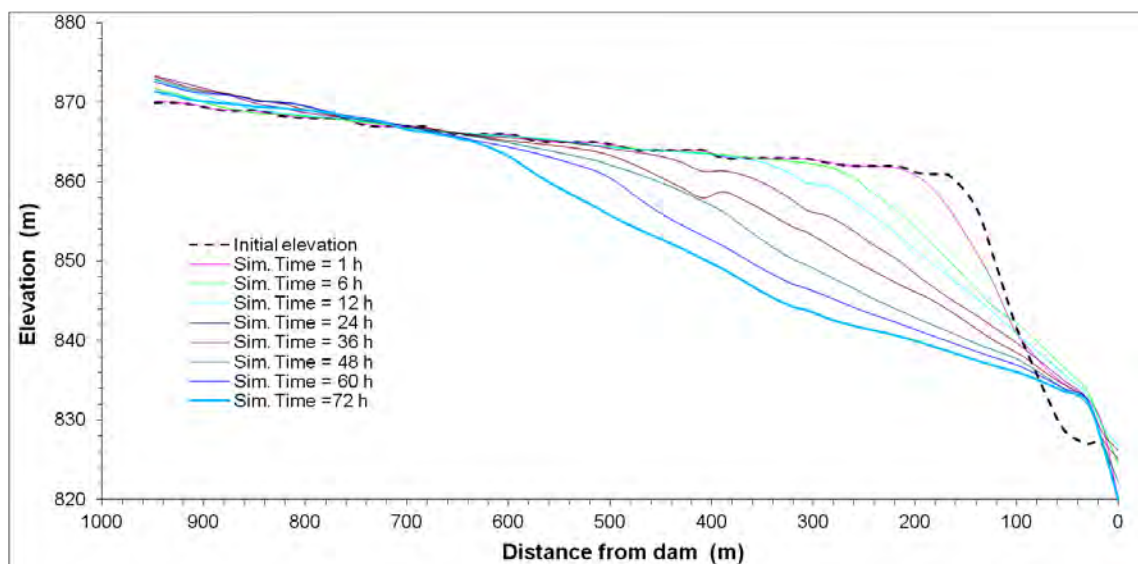


Figure 8. Evolution of the level of sediments during a flushing period of 72 hours.

The following two scenarios were considered: Initial water level at reservoir located at elevation 860 and 918 m. The erosion showed maximum values of 21 meters after 72 hours of washing in the first stage and approximately 45 meters in the second stage. These maximum values were reached at a distance of 100-200 meters upstream from the dam, where the maximum velocities occurred.

After a flushing period of 72 hours that involved a water flow of $408.9 \text{ m}^3/\text{s}$, the sediment volume removed by the bottom outlets in each scenarios were respectively 1.77 hm^3 and 3.51 hm^3 . In the first scenario, 100% of the sediments from the reservoir were swept, while in the second stage 81% were removed. These differences are due to the initial sedimentation volumes existing in each case. Considering the initial water level at the reservoir of 860 m, Figure 9 shows the relationship between the wash volume, the time, and the evolution of sediment removed through the bottom outlets. After a flushing period of 72 hours, a sediment volume equivalent to 1.77 hm^3 may be mobilized (value slightly greater than the initial deposition of 1.33 hm^3). During the initial emptying of the reservoir, higher rates of sediment transport appeared ($23 \text{ m}^3/\text{s}$ of sediments). Due to the occlusion of the outlets by the presence of a strong sediment load, the sediment transport falls below $3 \text{ m}^3/\text{s}$, and later continues with a rate near to $7 \text{ m}^3/\text{s}$. Except in the initial instants, the bottom outlets work in free surface conditions.

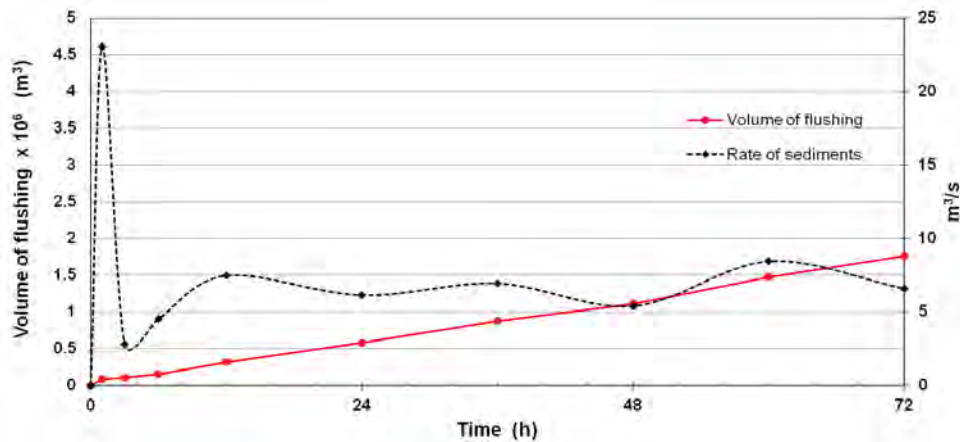


Figure 9. Evolution of the volume of sediments and the sediments transport through the bottom outlets during the flushing operation.

Three-dimensional simulation. The computational fluid dynamics (CFD) program FLOW-3D, which solves the Navier-Stokes equations discretized by finite differences, was used. It incorporates various turbulence models, a sediment transport model and an empirical model bed erosion (Guo, 2002; Mastbergen and Von den Berg, 2003; Brethour and Burnham, 2011), together with a method for calculating the free surface of the fluid without solving the air component (Hirt and Nichols, 1981).

The detailed operation of the bottom outlets, starting from the initial conditions of sedimentation obtained with the HEC-RAS program, was analyzed. Figure 10a shows the velocity vectors of the flow passing through the bottom outlets. The two outlets on the left side obtained a higher flow than the expected rate in the design ($Q = 102.22 \text{ m}^3/\text{s}$ for each outlet), while the two outlets on the right worked with a lower flow than expected.

Figure 10b shows the discharge flow at each bottom outlet, together with the total flow discharged and the mean flow discharged by each conduct for the first 3000 s of simulation. Outlets worked in a pressured and unsteady regime at the initial emptying of the reservoir, reaching a discharge near $1000 \text{ m}^3/\text{s}$. After the steady regime was reached (around 230 s of simulation), there was a free surface flow and the discharged flow was the expected ($408.90 \text{ m}^3/\text{s}$ during the flushing operation).

Figure 11 shows the erosion of sediment in the reservoir before the operation (initial condition) and after four hours of operation. Although the operation time was small (6 h), the sediment removed in the 3D operation was significant. This matched the results obtained in the 2D simulation, when the main washing rates occurred at the beginning.

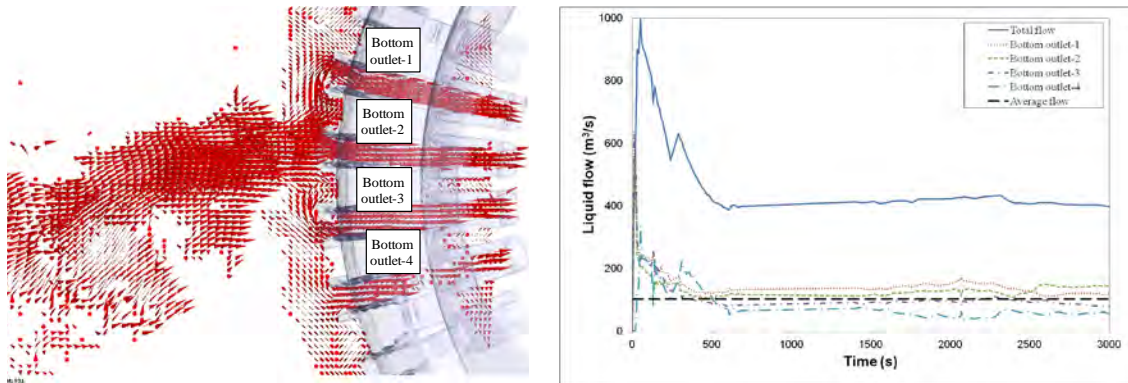


Figure 10. Bottom outlets: a) Velocity vectors after 5000 s of simulation. b) Total and partial flow through each bottom outlet during 5000 s of simulation.

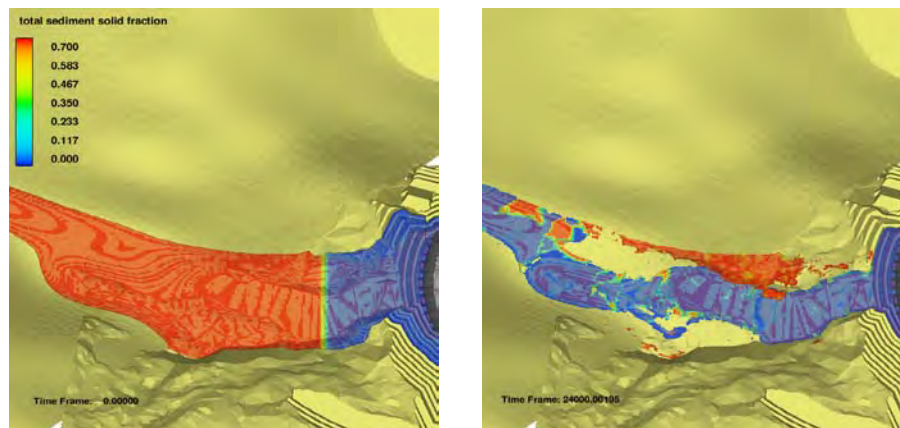


Figure 11. Initial and intermediate flushing of the sediments delta.

The bottom-left-central outlet received a more significant flow ($Q = 136.68 \text{ m}^3/\text{s}$) than the others. The flow near the inlet of the conduct could work alternately under pressure and free surface. Sediment levels were the lowest of the four outlets (Figure 12a). The opposite occurs in the outlet on the right. It has a lower flow ($Q = 56.78 \text{ m}^3/\text{s}$) and operates in free surface with a high level of sediment (Figure 12b).

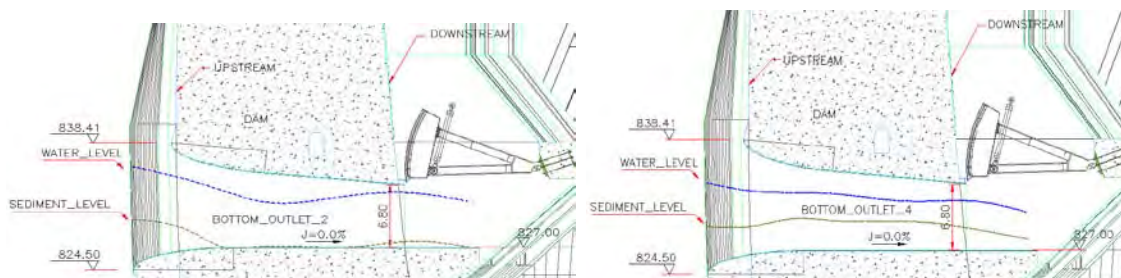


Figure 12. Levels of free surface water and sediment through the bottom outlet after 5000 s of simulation: a) Bottom outlet-2, $Q = 136.68 \text{ m}^3/\text{s}$; b) Bottom outlet-4, $Q = 56.78 \text{ m}^3/\text{s}$.

Table 2 shows the differences between the bottom outlets after 5000 s of simulation. Bottom outlet-2 has the greatest discharged flow and sediment removed, while bottom outlet-4 is the less efficient.

Besides this, as both ducts work with a significant water depth each could work well under pressure conditions.

Table 2. Flow water and sediment rate per each bottom outlet after 5000 s of simulation.

Bottom outlet	1	2	3	4	Total
Liquid flow (m ³ /s)	126.17	136.68	89.27	56.78	408.90
Maximum depth in the duct (m)	2.20	3.00	1.00	3.20	-
Sediment flow (ton/s)	4.48	6.18	4.20	2.95	17.81

Figure 13 shows the volume of sediment removed and the transient sediment transport during the first six hours of operation. Like in the two-dimensional simulation, there is significant sediment transport at the beginning of the simulation, with a maximum of 60 m³/s near the first hour (almost three times the two-dimensional results). Later, sediment the transport rate tends to decrease until near 6 m³/s which is similar to the two-dimensional result. The total volume of sediment calculated by FLOW-3D is much higher than with Iber program due to the that the simulations of the flushing phenomenon are very different in the first three hours.

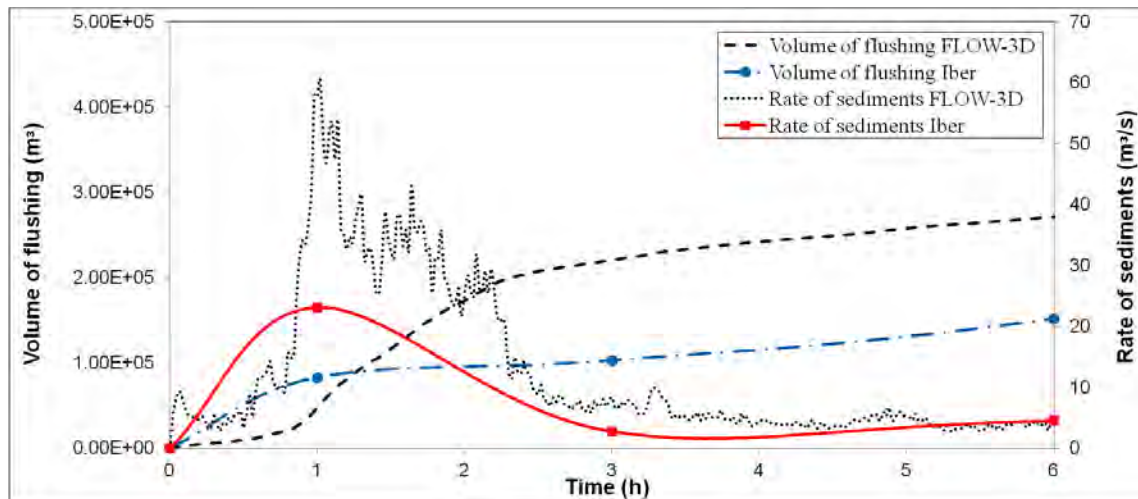


Figure 13. Flushing operation simulated with three-dimensional program.

CONCLUSION

In this paper, the complex phenomenon of flushing has been analyzed by using four interrelated methodologies: empirical formulations, one-dimensional simulations, two-dimensional simulations and three-dimensional simulations. Empirical simulations constitute an upper envelope of the sediment transport capacity. This procedure allowed an estimate of the coefficients of resistance or Manning roughness applied in the numerical simulations.

Due to the time period (one year) required to analyzing the sedimentation process in the reservoir, and the length of the reach (23.128 km), simulations were carried out with a one-dimensional program (two and three-dimensional programs need high-capacity equipment and long simulation times). Flushing operation was simulated with two-dimensional (Iber) and three-dimensional (FLOW-3D) programs. For 72 hours of flushing simulation, the Iber program required near 24 hours (Intel Core i7 CPU, 3.40 GHz processor, 16 GB RAM and 8 cores). The FLOW-3D program, by using the same equipment, would require more than 960 h. Hence, the three-dimensional simulations were only used to analyze the behavior of the flow in the first 6 h of the flushing (264 h of simulation).

The results demonstrated the suitability of crossing different methodologies to achieve an adequate resolution of complex phenomena such as flushing operations. Thus, numerical simulations of differing degrees of complexity were used to complement the classical formulations and allow a better understanding of the physical phenomena.

ACKNOWLEDGMENTS

The authors are grateful to CELEC EP - Hidropaute and the Consorcio POYRY-Caminosca Asociados for the data provided.

REFERENCES

- Brethour, J., and Burnham, J. (2010). "Modeling Sediment Erosion and Deposition with the FLOW-3D Sedimentation & Scour Model". Flow Science Technical Note, FSI-10-TN85, 1-22.
- Castillo, L., Marín, M. D., and Lima, P. R. (2009a). "Coeficientes de resistencia, transporte de sedimentos y caudal dominante en regiones semiáridas". *I Jornadas Ingeniería del Agua, JIA*. Madrid.
- Castillo, L., Martín Vide, J. P., and Marín, M. D. (2009b). "Coeficientes de resistencia, transporte de sedimentos y caudal dominante en regiones semiáridas." *I Jornadas de Ingeniería del Agua, JIA*. Madrid.
- Castillo, L., and Marín, M. D. (2010). "Caracterización hidrológica e hidráulica en regiones semiáridas." *XXIV IAHR*, Punta del Este, Uruguay.
- Castillo, L., and Marín, M. D. (2011). "Characterization of Ephemeral Rivers." *34th IAHR World Congress*. Brisbane. Australia.
- Einstein, H. A., and Barbarossa, N. L. (1952). "River Channels Roughness." *ASCE*, 117, 1121-1132.
- Fuentes, R., and Aguirre-Pe, J. (1991). "Resistance to flow in steep rough streams." *J. Hydraulic Engineering*, 116(11), 1374-1387.
- Guo, J. (2002). Hunter Rouse and Shields diagram, *Proc 1th IAHR-APD Congress*, Singapore, 2, 1069-1098.
- Heredia, E., Buitrón, R., Panchi, P., Calo, J., and Lara, C. (2012). "Estudio mediante modelación matemática de la sedimentación y lavado de sedimentos mediante flushing en el embalse Maduriacu." *XXV Congreso Latinoamericano de Hidráulica*, San José, Costa Rica.
- Hirt, C. W., and Nichols, B. D. (1981). "Volume of Fluid (VOF) Method for the Dynamics of Free Boundaries." *Journal of Computational Physics*, 39 (201).
- Janssen, R. (1999). *An Experimental Investigation of Flushing Channel Formation during Reservoir Drawdown*. Dissertation presented to the University of California at Berkeley, in partial fulfillment for the requirements for the degree of Doctor of Philosophy.
- Lai, J. S., Shen, H. W. (1996). "Flushing sediment through reservoirs." *J. Hydraulic Research*, 24 (2).
- Mahmood, K. (1987). "Reservoir Sedimentation: Impact, Extent, and Mitigation." World Bank Technical Paper Number 71, *The International Bank for Reconstruction and Development*.
- Marín, M. D., and Castillo, L. (2011). "Simulación agregada-distribuida y evaluación del transporte de sedimentos en cauces efímeros." *II Jornadas Sobre Ingeniería del Agua*, Barcelona, España.
- Mastbergen, D. R. and Von den Berg J. H. (2003). "Breaching in fine sands and the generation of sustained turbidity currents in submarine canyons." *Sedimentology*, 50, 625-637.
- Meyer-Peter, E., and Müller, R. (1948). "Formulations of the Bed-load Transport." *Proc. of the II IAHR*, Stockholm, 39-64.
- Van Rijn, L. C. (1986). *Manual sediment transport measurements in rivers, estuaries and coastal seas*. Rijkswaterstaat y Aqua publications.
- Van Rijn, L. C. (1987). *Mathematical modelling of morphological processes in the case of suspended sediment transport*. Delft Hydraulics Communication No. 382.
- Yang, S. Q. (2005). "Sediment Transport Capacity." *J. Hydraulic Research*, 43(1), 12-22.
- Yang, C. T. (1996). *Sediment Transport: Theory and Practice*. McGraw-Hill International Ed., NY, USA.